Supporting Information for

First-Principles Calculation of ^{11}B Solid-State NMR Parameters of Boron-Rich Compounds II: The Orthorhombic Phases MgB_7 and $MgB_{12}C_2$ and the Boron Modification γ-B_{28}

Martin Ludwig[a] and Harald Hillebrecht[a,*]

[a] *Institut für Anorganische und Analytische Chemie, Albert-Ludwigs-Universität 79104 Freiburg, Germany*

[*] E-mail: harald.hillebrecht@ac.uni-freiburg.de;
Phone: +49 (0)761 2036131;
Fax: +49 (0)761 2036012

Table S1: Lattice parameters of primitive cells used for the calculations.[a]

	length (Å)			angles (°)			volume (Å^3)
compound	a	b	c	α	β	γ	
MgB_7	10.4782	5.9769	7.2719	65.735	43.908	90.000	254.4
o-$MgB_{12}C_2$	5.6133	9.8280	6.9107	44.678	66.038	90.000	218.8

[a] for γ-B_{28} lattice parameters of primitive cell correspond to conventional orthorhombic cell.

Table S2: Structure parameters in terms of the orthorhombic axes before and after relaxation.

			start			relaxed		
compound	site	Wyckoff position	$\bar{x}$	$\bar{y}$	$\bar{z}$	$\bar{x}$	$\bar{y}$	$\bar{z}$
MgB_7	B(1)	8i	0.58356	0.75000	0.22495	0.58384	0.75000	0.22560
	B(2)	16j	0.68650	0.59402	0.08645	0.68641	0.59432	0.08680
	B(3)	16j	0.82803	0.50276	0.20540	0.82772	0.50337	0.20522
	B(4)	8i	0.83263	0.75000	0.07391	0.83208	0.75000	0.07394
	B(5)	8i	0.39129	0.25000	0.36547	0.38985	0.25000	0.36597
	Mg(1)	4a	0.00000	0.50000	0.00000	0.00000	0.50000	0.00000
	Mg(2)	4e	0.00000	0.25000	0.38430	0.00000	0.25000	0.38423
o-$MgB_{12}C_2$	B(1)	8h	0.00000	0.33274	0.02107	0.00000	0.33303	0.02066
	B(2)	16j	0.16176	0.43614	0.16054	0.16150	0.43627	0.16042
	B(3)	16j	0.76069	0.91504	0.44807	0.76053	0.91501	0.44795
	B(4)	8h	0.50000	0.90606	0.31860	0.50000	0.90637	0.31848
	C	8h	0.50000	0.83785	0.12929	0.50000	0.83785	0.12909
	Mg	4e	0.00000	0.25000	0.36187	0.00000	0.25000	0.36041
γ-B_{28}	B(1)	4g	0.33620	0.50760	0.00000	0.33570	0.50771	0.00000
	B(2)	8h	0.83910	0.71890	0.87370	0.83904	0.71918	0.87478
	B(3)	8h	0.15390	0.59380	0.79240	0.15301	0.59300	0.79215
	B(4)	4g	0.64690	0.72840	0.50000	0.64779	0.72925	0.50000
	B(5)	4g	0.66900	0.98230	0.00000	0.66966	0.98090	0.00000

Table S3: Chemical shift parameters δ_{iso}, δ_{csa} in ppm and η_{cs} without macroscopic correction of magnetic susceptibility[a] together with corresponding susceptibilies χ.[1] All values according to PAW PPs.

		without correction[a]			$-\chi$	
compound	site	δ_{iso}	δ_{csa}	η_{cs}	$((8\pi/3)\,\mathrm{ppm})$	$(10^{-6}\,\mathrm{cm}^3/\mathrm{mol})$
MgB_7	B(1)	11.9	12.9	0.22	13.4	244.4
	B(2)	23.4	18.2	0.93		
	B(3)	27.3	17.4	0.97		
	B(4)	49.2	2.4	0.35		
	B(5)	−20.9	15.0	0.23		
o-$MgB_{12}C_2$	B(1)	1.1	18.2	0.23	13.9	219.2
	B(2)	10.0	−14.9	0.97		
	B(3)	24.4	−11.2	0.49		
	B(4)	50.4	−10.7	0.54		
γ-B_{28}	B(1)	17.7	−13.5	0.94	15.8	225.6
	B(2)	7.6	−25.9	0.90		
	B(3)	21.4	10.2	0.70		
	B(4)	23.3	−11.4	0.09		
	B(5)	23.4	20.3	0.66		

[a] correction term given by $\sigma(\mathbf{G}=\mathbf{0}) = -(8\pi/3)\chi$.[2]

Table S4: Parameters used for spectrum simulation (beside PAW calculated values) with relative intensity I, gaussian/lorentzian width w, approximated relative area A and occupied site multiplicity. Overall distribution of gaussian to lorentzian line type was assumed to be 50 %.

compound	site	I (%)	w (ppm)	A (%)	occ. (%)
MgB_7	B(1)	10.8	8.0 ± 1.4	13.0 ± 2.3	14.3
	B(2)	13.8	14.0 ± 0.6	28.0 ± 1.2	28.6
	B(3)	13.8	14.0 ± 0.6	28.0 ± 1.2	28.6
	B(4)	34.9	3.0 ± 0.9	15.0 ± 4.4	14.3
	B(5)	26.7	4.0 ± 0.1	16.0 ± 0.5	14.3
o-$MgB_{12}C_2$	B(1)	5.6	33.0 ± 11.5	18.0 ± 6.4	16.7
	B(2)	24.4	13.0 ± 1.2	31.0 ± 2.8	33.3
	B(3)	33.8	10.0 ± 0.1	33.0 ± 0.4	33.3
	B(4)	36.1	5.0 ± 0.2	18.0 ± 0.9	16.7

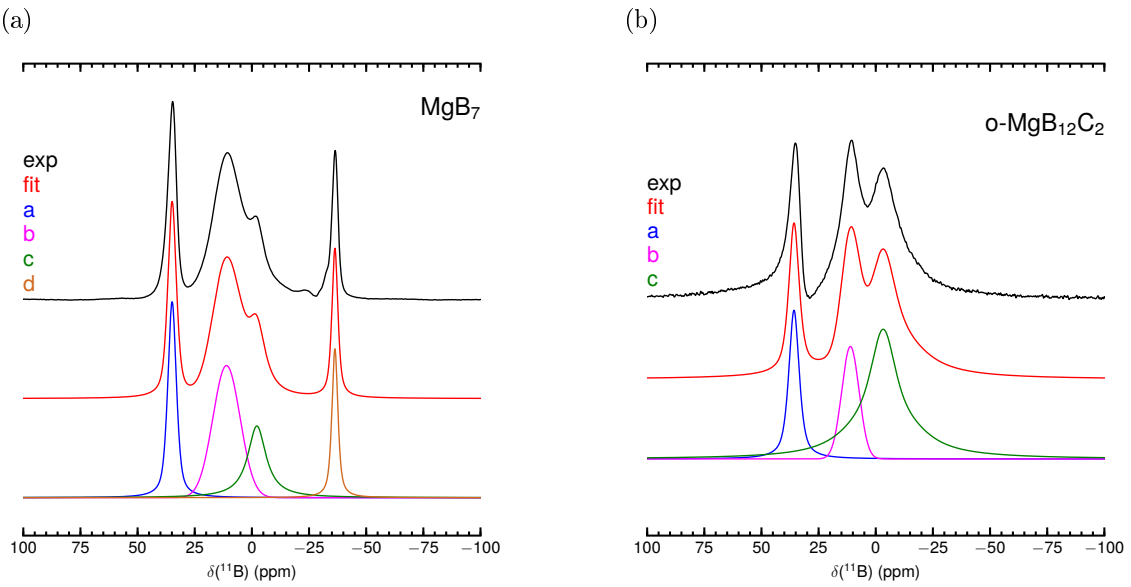

Figure S1: Central transition fits applying the "Gaus/Lor" model in the DMfit program[3] to the recorded spectra of (a) MgB_7 and (b) o-$MgB_{12}C_2$: For MgB_7 we obtain $I_a : I_b : I_c : I_d = 35.7 \pm 0.2\,\% : 24.1 \pm 0.1\,\% : 13.1 \pm 0.2\,\% : 27.1 \pm 0.2\,\%$, the shifts $\delta^a_{ctf} = 34.9\,\text{ppm} \pm 0.2\,‰$, $\delta^b_{ctf} = 11.1\,\text{ppm} \pm 2.8\,‰$, $\delta^c_{ctf} = -2.2\,\text{ppm} \pm 25.6\,‰$, $\delta^d_{ctf} = -36.3\,\text{ppm} \pm 0.3\,‰$, the widths $w_a = 4.4\,\text{ppm} \pm 0.6\,\%$, $w_b = 14.0\,\text{ppm} \pm 0.5\,\%$, $w_c = 9.6\,\text{ppm} \pm 2.0\,\%$, $w_d = 3.1\,\text{ppm} \pm 1.1\,\%$ with the distribution of gaussian compared to lorentzian line type $x_a = 44\,\%$, $x_b = 100\,\%$ (full gaussian), $x_c = 0\,\%$ (full lorentzian) and $x_d = 32\,\%$; For o-$MgB_{12}C_2$ the fit yields $I_a : I_b : I_c = 38.0 \pm 0.5\,\% : 28.8 \pm 0.5\,\% : 33.2 \pm 0.4\,\%$, the shifts $\delta^a_{ctf} = 35.8\,\text{ppm} \pm 0.9\,‰$, $\delta^b_{ctf} = 11.1\,\text{ppm} \pm 5.7\,‰$, $\delta^c_{ctf} = -3.3\,\text{ppm} \pm 34.3\,‰$, the widths $w_a = 5.4\,\text{ppm} \pm 2.1\,\%$, $w_b = 8.9\,\text{ppm} \pm 1.8\,\%$, $w_c = 16.8\,\text{ppm} \pm 2.4\,\%$ with the distribution of gaussian compared to lorentzian line type $x_a = 34\,\%$, $x_b = 100\,\%$ (full gaussian) and $x_c = 33\,\%$.

Table S5: Euler angles α, β and γ in ° correspond to the calculated magnetic shielding principal axis system relative to the principal axis system of the electric field gradient tensor obtained by MagresView.[4] Values follow the ZYZ convention according to the book of M. E. Rose, Elementary Theory of Angular Momentum, Wiley, New York, 1957.

		NC			PAW		
compound	site	α	β	γ	α	β	γ
MgB_7	B(1)	0	173	90	0	173	−90
	B(2)	−100	36	143	−101	35	144
	B(3)	−93	67	−92	−93	66	−92
	B(4)	179	162	−1	−180	72	0
	B(5)	−90	100	0	−90	100	0
o-$MgB_{12}C_2$	B(1)	90	138	−180	90	138	−180
	B(2)	129	87	−44	130	88	−43
	B(3)	17	99	−100	19	99	−102
	B(4)	180	22	0	180	21	0
γ-B_{28}	B(1)	90	106	90	90	106	90
	B(2)	101	60	−138	100	58	−136
	B(3)	−119	91	116	−121	90	117
	B(4)	90	101	90	90	101	90
	B(5)	90	35	180	90	34	−180

Table S6: Additional information of geometry related angles (Table 6 of the manuscript) in ° with root-mean-square deviation (rmsd) θ_{rmsd} of θ_{av} and θ'_{rmsd} of θ'_{av}, respectively. All values correspond to optimized geometry.

compound	site	θ_{rmsd}	θ'_{rmsd}
MgB_7	B(1)	1.35	1.22
	B(2)	0.93	0.86
	B(3)	1.27	0.98
	B(4)	0.79	0.46
o-$MgB_{12}C_2$	B(1)	0.77	0.70
	B(2)	1.14	0.87
	B(3)	0.59	0.36
	B(4)	1.13	0.56
γ-B_{28}	B(1)	0.22	0.24
	B(2)	0.67	0.32
	B(3)	0.33	0.30
	B(4)	0.63	0.19
$(B_{12}H_{12})^{2-}$		0.00	0.00

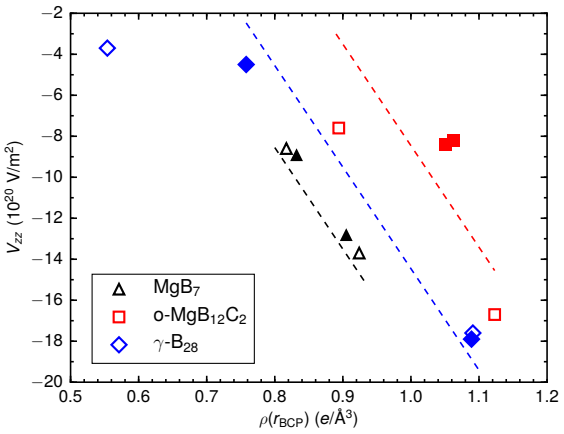

Figure S2: Values of the EFG main component V_{zz} from PAW calculations plotted against $\rho(r_{\mathrm{BCP}})$ of B sites B(1) to B(4) in the icosahedral B_{12} units with data from Tables 3 and 6 of the manuscript. The properties of the BCPs are associated with the exohedral bonds and in accordance to the orientation of the V_{zz} axis. Filled squares correspond to properties of sites bonded to the interstitial unit. The trend lines are meant to guide the eye.

References

[1] F. Mauri and S. G. Louie, *Phys. Rev. Lett.*, 1996, **76**, 4246–4249.

[2] F. Mauri, B. G. Pfrommer and S. G. Louie, *Phys. Rev. Lett.*, 1996, **77**, 5300–5303.

[3] D. Massiot, F. Fayon, M. Capron, I. King, S. Le Calvé, B. Alonso, J.-O. Durand, B. Bujoli, Z. Gan and G. Hoatson, *Magn. Reson. Chem.*, 2002, **40**, 70–76.

[4] S. Sturniolo, T. F. Green, R. M. Hanson, M. Zilka, K. Refson, P. Hodgkinson, S. P. Brown and J. R. Yates, *Solid State Nucl. Mag.*, 2016, **78**, 64–70.